WACV #2648

Blind Image Deblurring with FFT-ReLU Sparsity Prior: Supplementary Material

Anonymous WACV Algorithms Track submission

Paper ID 2648

1. Closed-form Solution for I

In our algorithm, the blind deconvolution section involves estimating the nonlinear RFT(I). This is done by using a linear operator F, such that FI = RFT(I). The computation of F is done using gradient descent with Adam optimizer.

Given F, we can solve for I from:

$$\min_I ||\mathbf{T}_k\mathbf{I} - \mathbf{B}||_2^2 + \gamma||\nabla \mathbf{I} - \mathbf{g}||_2^2 + \beta||\mathbf{F}\mathbf{I} - \mathbf{h}||_2^2 \tag{1}$$

where $\mathbf{T}_k$ is a Toeplitz matrix of k, which is multiplied with vectors using FFT **B, g** and **u** are denoted in their vector forms, respectively.

The solution for Equation (1) is computed as follows:

$$\begin{aligned}L &= \min_I ||\mathbf{T}_k\mathbf{I} - \mathbf{B}||_2^2 + \gamma||\nabla \mathbf{I} - \mathbf{g}||_2^2 + \beta||\mathbf{F}\mathbf{I} - \mathbf{h}||_2^2 \\ &= (\mathbf{T}_k\mathbf{I} - \mathbf{B})^T(\mathbf{T}_k\mathbf{I} - \mathbf{B}) + \gamma(\nabla\mathbf{I} - \mathbf{g})^T(\nabla\mathbf{I} - \mathbf{g}) + \\ &\beta(\mathbf{F}\mathbf{I} - \mathbf{h})^T(\mathbf{F}\mathbf{I} - \mathbf{h}) \\ &= \mathbf{I}^T\mathbf{T}_k^T\mathbf{T}_k\mathbf{I} - \mathbf{I}^T\mathbf{T}_k^T\mathbf{B} - \mathbf{B}\mathbf{T}_k^T\mathbf{I} + \mathbf{B}^T\mathbf{B} + \gamma\mathbf{I}^T\nabla^T\nabla I - \\ &\gamma\mathbf{I}^T\nabla^T g - \gamma\mathbf{g}^T\nabla\mathbf{I} + \gamma\mathbf{g}^T\mathbf{g} + \beta\mathbf{I}^T\mathbf{F}^T\mathbf{F}\mathbf{I} - \beta\mathbf{I}^T\mathbf{F}^T\mathbf{h} - \\ &\beta\mathbf{h}^T\mathbf{F}\mathbf{I} + \beta\mathbf{h}^T\mathbf{h}\end{aligned} \tag{2}$$

Here, $\nabla = (\nabla_x, \nabla_y)$ represents the matrix for computing axiswise gradients. Differentiating Equation (2) with respect to I , we get:

$$\begin{aligned}\frac{dL}{dI} &= 2\mathbf{T}_k^T\mathbf{T}_k\mathbf{I} - \mathbf{T}_k^T\mathbf{B} - \mathbf{T}_k^T\mathbf{B} + 0 + 2\gamma\nabla^T\nabla I - \gamma\nabla^T\mathbf{g} - \\ &\gamma\nabla^T\mathbf{g} + 0 + 2\beta\mathbf{F}^T\mathbf{F}\mathbf{I} - \beta\mathbf{F}^T\mathbf{h} - \beta\mathbf{F}^T\mathbf{h} \\ &= 2\mathbf{T}_k^T\mathbf{T}_k\mathbf{I} - 2\mathbf{T}_k^T\mathbf{B} + 2\gamma\nabla^T\nabla I - 2\gamma\nabla^T\mathbf{g} + 2\beta\mathbf{F}^T\mathbf{F}\mathbf{I} \\ &- 2\beta\mathbf{F}^T\mathbf{h}\end{aligned} \tag{3}$$

In the case of convergence, $\frac{dL}{dI} = 0$. Therefore,

$$\begin{aligned}\mathbf{I} &= \frac{\mathbf{T}_k^T\mathbf{B} + \gamma\nabla^T\mathbf{g} + \beta\mathbf{F}^T\mathbf{h}}{\mathbf{T}_k^T\mathbf{T}_k + \gamma\nabla^T\nabla + \beta\mathbf{F}^T\mathbf{F}} \\ &= \mathcal{F}^{-1}\left(\frac{\overline{\mathcal{F}(\mathbf{K})}\mathcal{F}(\mathbf{B}) + \gamma\overline{\mathcal{F}(\nabla)}\mathcal{F}(\mathbf{g}) + \beta\overline{\mathcal{F}(\mathbf{F})}\mathcal{F}(\mathbf{h})}{\overline{\mathcal{F}(\mathbf{K})}\mathcal{F}(\mathbf{K}) + \gamma\overline{\mathcal{F}(\nabla)}\mathcal{F}(\nabla) + \beta\overline{\mathcal{F}(\mathbf{F})}\mathcal{F}(\mathbf{F})}\right)\end{aligned} \tag{4}$$

This is the closed-form solution presented in our paper.

2. Parameter Sensitivity

As mentioned in the text, for the variable λ, we experimented with some other values to find the optimum, with respect to kernel similarity (defined as SSIM between the estimated kernel and ground-truth kernel).

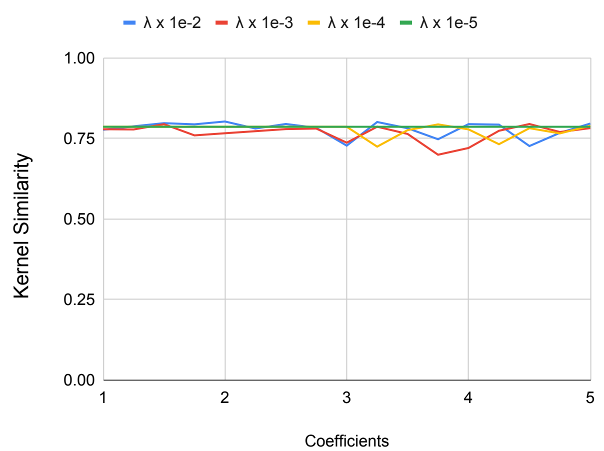

Figure 1. Finding Optimum Value of λ

In Fig. 1, we can see that for ranges in 10^{-3}, the kernel similarity is lower. In ranges 10^{-4} and 10^{-5}, the levels of kernel similarity are similar. However, in our experiments, using values around 10^{-5} increased the runtime of our algorithm. Therefore, we chose 3×10^{-4} since it provided the best results. For μ, we conducted similar experiments and found the optimum value.

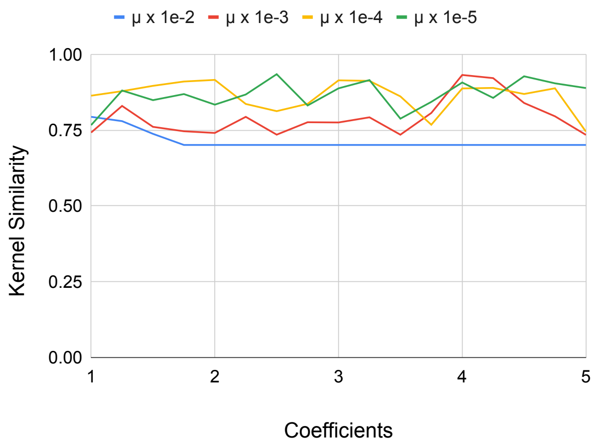

Figure 2. Finding Optimum Value of μ

We can see from the experiment results in Fig. 2 that the highest levels of kernel similarity are achieved in the ranges of 10^{-3}, and we set the value of μ to 0.004.

3. More Experimental Results

In this section, we show more results of our algorithm on input blurry images. We present them as input and output image pairs, and the estimated blur kernel from our algorithm is embedded into the top right corner of the output image. The images are obtained from datasets provide by Lai *et al*. [1] and Levin *et al*. [2].

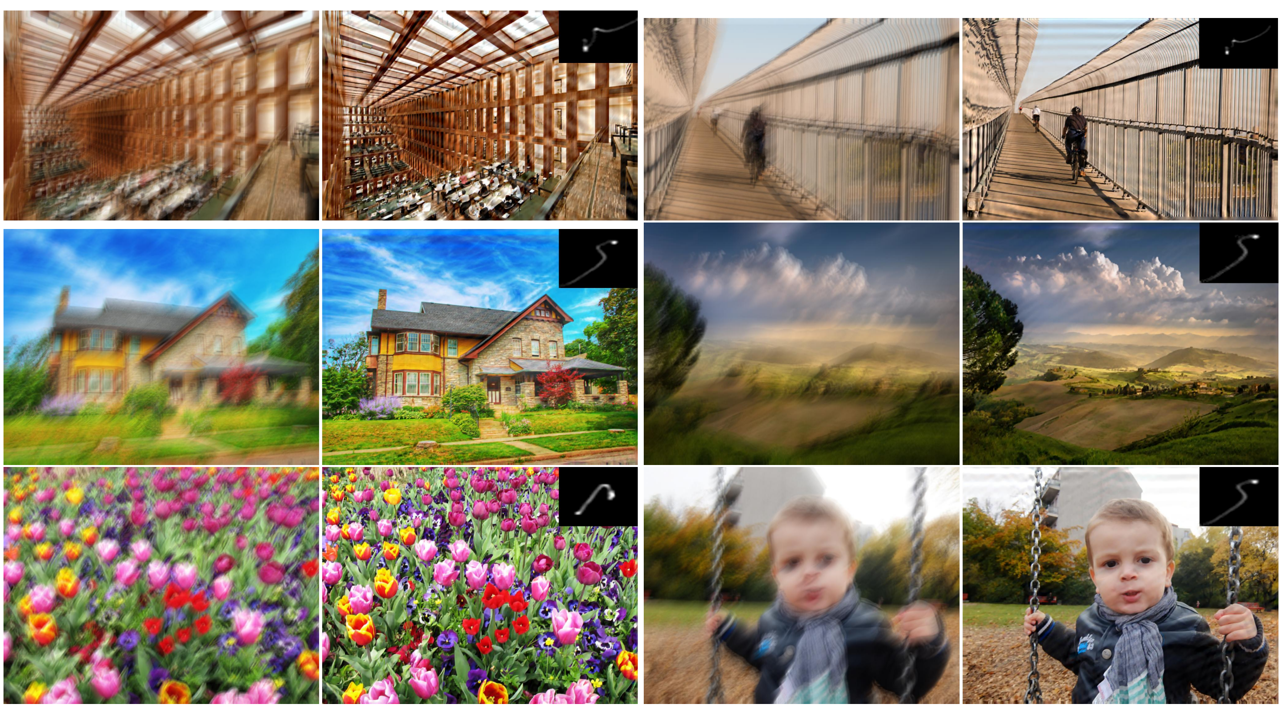

Figure 3. Results of our blind image deblurring algorithm, presented with the corresponding estimated blur kernel. For each pair, the input image is on the left, and the output of our algorithm is on the right.

Figure 4. More results of our blind image deblurring algorithm, presented with the corresponding estimated blur kernel. For each pair, the input image is on the left, and the output of our algorithm is on the right for each pair.

References

[1] Wei-Sheng Lai, Jia-Bin Huang, Zhe Hu, Narendra Ahuja, and Ming-Hsuan Yang. A comparative study for single image blind deblurring. In *IEEE Conferene on Computer Vision and Pattern Recognition*, 2016. 2

[2] Anat Levin, Yair Weiss, Fredo Durand, and William T. Freeman. Understanding and evaluating blind deconvolution algorithms. In *2009 IEEE Conference on Computer Vision and Pattern Recognition*, pages 1964–1971, 2009. 2